Journal of The Electrochemical Society, **154** (5) H331-H335 (2007)
0013-4651/2007/154(5)/H331/5/$20.00 © The Electrochemical Society

Polymer/AlO_x Bilayer Dielectrics for Low-Voltage Organic Thin-Film Transistors

Jeong-M. Choi,[a] D. K. Hwang,[a] S. H. Jeong,[a] Ji Hoon Park,[b] Eugene Kim,[b] Jae Hoon Kim,[a] and Seongil Im[a,z]

[a]*Institute of Physics and Applied Physics, Yonsei University, Seoul 120-749 Korea*
[b]*Department of Information and Display, Hongik University, Seoul 121-791 Korea*

We report on the low-voltage-driven organic thin-film transistors (OTFTs) with various organic films [pentacene, tetracene, and copper-phthalocyanine (CuPc)] for the semiconductor channel on a thin poly-4-vinylphenol (PVP)/aluminum oxide (AlO_x) bilayer gate dielectric. Quite a large capacitance of 31 nF/cm^2 and a high dielectric strength of ~4 MV/cm were achieved from the 45 nm thin polymer/100 nm thick $A1O_x$ bilayer dielectric. All the organic channel layers deposited on the bilayer exhibited good crystalline quality as characterized by both X-ray diffraction (XRD) and atomic force microscopy (AFM) surface imaging because the bilayer had a smoothened and hydrophobic PVP surface on top. Our OTFTs with the bilayer dielectric exhibited good field-effect mobilities of 0.55, 0.07, and 0.004 cm^2/V s for pentacene, tetracene, and CuPc channels, respectively, at a low operating voltage of less than −8 V.
 [DOI: 10.1149/1.2667492]

Manuscript submitted October 19, 2006; revised manuscript received December 18, 2006.
Available electronically March 12, 2007.

Organic thin-film transistors (OTFTs) have been extensively studied due to their potential toward driving circuits for display or low-cost logic applications.[1-3] For a good OTFT unit device, a considerable amount of research work has focused on the dielectrics (gate insulators), adjoining organic semiconductor active channels, and source/drain (S/D) electrodes.[4-10] Among these, the most important is, in general, a good gate dielectric with a high capacitance, high dielectric strength, and a well-accommodating surface for organic crystalline channel growth. Researchers have already realized low-voltage operations of pentacene TFTs with high-*k* inorganic dielectrics or ultrathin organic dielectrics,[4] while we recently succeeded in adopting thin organic polymer layers on an inorganic high-*k* layer to retain the advantages from both low-*k* organic and high-*k* inorganic: good pentacene growth on a hydrophobic polymer surface[5,11] and considerable capacitance from the high-*k* inorganic. According to the previous results from pentacene TFTs with a thin polymer/high-*k* yttrium oxide (YO_x) bilayer dielectric, quite a high field-effect mobility of more than 1.5 cm^2/V s can be achieved without any serious gate leakage.[11]

In the present study we have fabricated low-voltage high-performance OTFTs adopting a thin poly-4-vinylphenol (PVP)/aluminum oxide (AlO_x) bilayer for a gate dielectric with two research objectives: examining the properties of a PVP/AlO_x bilayer dielectric in detail and combining them with various important organic semiconductors of pentacene, tetracene, and copper-phthalocyanine (CuPc), which are to be used for the channels of low-voltage OTFTs.

Experimental

Prior to the deposition of an AlO_x film on indium-tin-oxide (ITO) glass, the glass was cleaned with acetone, ethanol, and deionized water, in that order. After that, 100 nm thick AlO_x films were deposited on the ITO glass by radio frequency (rf) magnetron sputtering in a vacuum chamber at room temperature (the initial base pressure was about 2×10^{-6} Torr and the working Ar pressure was fixed at 20 mTorr). The thickness and sheet resistance of the ITO films were 79 nm and 30 Ω/□, respectively. PVP films on the AlO_x layer were then prepared to a thickness of 45 nm by spin coating of PVP/poly (melamine-co-formaldehyde) solutions with a cross-linking agent of propylene glycol monomethyl ether acetate (PGMEA) and by subsequent cross-linking (curing) at 175°C for 1 h in a vacuum oven. Then, organic (pentacene, tetracene, and CuPc) channels and S/D electrodes (Au) were sequentially patterned on the PVP/AlO_x bilayer dielectrics through shadow masks by thermal evaporation. The deposition rate was fixed to 0.1 nm/s during the evaporation of each organic channel material. These organic films were confirmed to be crystalline as measured by X-ray diffractometry (XRD, using Cu Kα

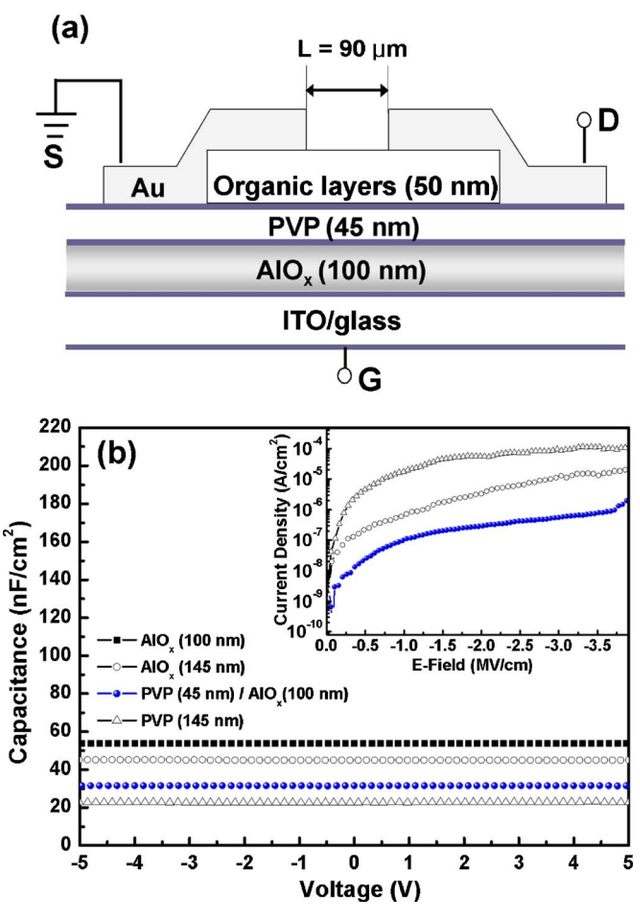

Figure 1. (Color online) (a) Schematic cross section of our OTFTs with the hybrid bilayer dielectric, (b) 1 MHz C–V characteristics measured from single AlO_x (100 and 145 nm) layers, PVP (45 nm)/AlO_x (100 nm) bilayer, and single PVP (145 nm) layer dielectric films. (Inset) J–E curves of the three different dielectric sets.

[z] E-mail: semicon@yonsei.ac.kr

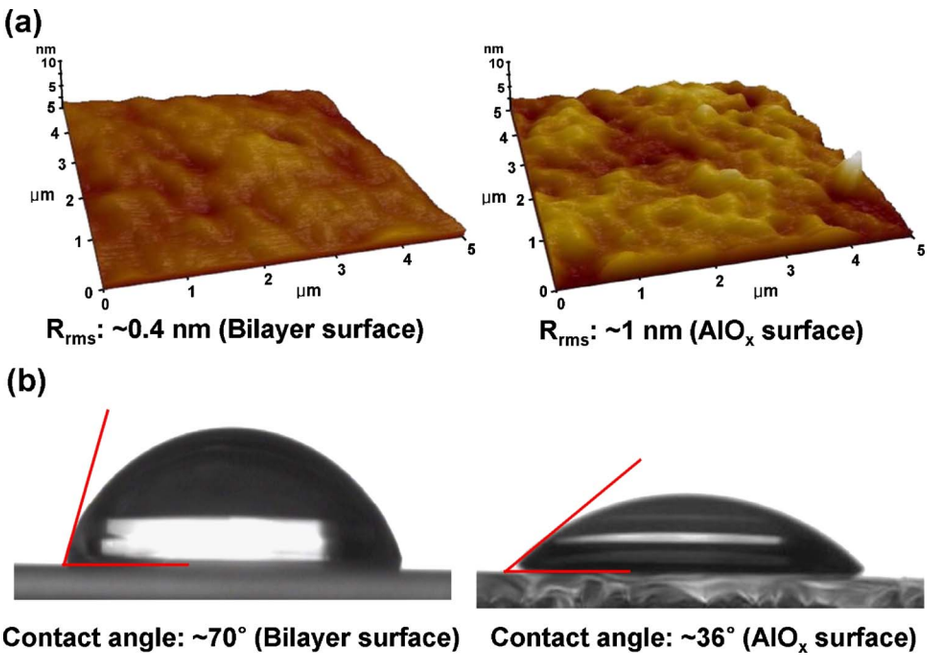

Figure 2. (Color online) (a) AFM surface images of the PVP (45 nm)/AlO_x 100 nm)/ITO glass (left) and the AlO_x (100 nm)/ITO glass substrates (right). The values of R_{rms} are ~0.4 and ~1 nm, respectively. (b) Contact-angle photographs of both dielectric films [(left) PVP/AlO_x/ITO: ~ 70° and (right) AlO_x/ITO: ~ 36°].

X-ray). The thicknesses of organic channels and Au were 50 and 100 nm, respectively. Figure 1a shows the schematic cross section of our TFT with a nominal channel length, L, of 90 μm and width, W, of 500 μm. The surface images of our organic channels and dielectric films were obtained with atomic force microscopy (AFM, model XE-100, PSIA).

All electrical characterizations were carried out with a semiconductor parameter analyzer (model HP 4155C, Agilent Technologies) and capacitance vs voltage (C–V) measurements were made with a HP 4284 capacitance meter (1 MHz). All measurements were carried out at room temperature.

Results and Discussion

Figure 1a shows the cross section of our device structure where organic films were employed as active layers on the PVP/AlO_x bilayer dielectric. Based on this organic–inorganic hybrid or bilayer approach, we tried to retain the following three advantages: maintaining a considerable dielectric capacitance supported by a high-k inorganic oxide, improving the dielectric strength usually low for AlO_x or PVP layer alone, and changing the dielectric surface state from rough hydrophilic inorganic to smooth hydrophobic organic for growth of high crystalline of active channels. Basically, the AlO_x is polar and thus should be very hydrophilic. PVP also has hydroxyl (OH-) groups and thus shows a strong hydrophilic chemical state on its surface after spin-casting. However, this hydroxyl group can be effectively removed forming water or methanol molecules when the PVP is well cross-linked through the condensation reaction, coupled with poly (melamine-*co*-formaldehyde).[12] As a result of this reaction, the cross-linked PVP film becomes denser in itself, smoother, and more hydrophobic in terms of its surface properties.[12]

In Fig. 1b, the C–V and current density vs electric field (J–E) relationship plots are displayed for single AlO_x layers (100 and 145 nm), a PVP (45 nm)/AlO_x (100 nm) bilayer, and a single PVP layer (145 nm) dielectric deposited on ITO glass substrates (we deposited 300 μm diam Au dots on top for these measurements). The dielectric capacitances of the single AlO_x layers (100 and 145 nm), PVP/AlO_x bilayer, and single PVP layer ($C_{100nm-AlO_x}$, $C_{145nm-AlO_x}$, $C_{bilayer}$, C_{PVP}) were measured to be about 54, 45, 31, and 23.5 nF/cm^2, respectively. Based on the measurement values of the single AlO_x layers and the PVP film, their dielectric constants, k_{AlO_x} and k_{PVP}, turned out to be about 6.5 and 3.8, respectively. Therefore, the capacitance of our thin PVP overlayer ($C_{thin\ PVP}$) in the bilayer can also be calculated by using the experimental values of $C_{100nm-AlO_x}$ and $C_{bilayer}$ as follows

$$C_{thin\ PVP} = \left(\frac{1}{C_{bilayer}} - \frac{1}{C_{100\ nm-AlO_x}} \right)^{-1} = 72.8\ \text{nF/cm}^2 \qquad [1]$$

The dielectric constant of our 45 nm thin PVP overlayer is then worked out to be ~3.7, which is very similar to the value obtained from the 145 nm thick single PVP, supporting that all of our experimental measurements, including layer thickness, were quite consistent. According to the J–E results shown in the inset of Fig. 1b, it is also noted that our bilayer dielectric approach is quite effective even in the aspects of dielectric strength and leakage current. Compared to the 145 nm thick single AlO_x layer and single PVP layer, our bilayer dielectric with the same total thickness exhibited much improved leakage current resistance. The dielectric strength of the bilayer was about 4 MV/cm in our leakage standard of 1×10^{-6} A/cm^2, while the strength of single AlO_x dielectric was about 1 MV/cm. In particular, the properties of the single PVP layer were too inferior to be applied to a gate dielectric for OTFT; its dielectric strength was only 0.25 MV/cm for the same leakage standard. The enhanced dielectric strength was achieved from our bilayer approach because the leakage current should serially go through two different materials which possess different leakage paths.

Figure 2a displays the AFM images of dielectrics surfaces [bilayer (left) and single AlO_x layer (right)]. The AlO_x layer showed a rough surface morphology with a root-mean-square (rms) roughness (R_{rms}) of ~1 nm, while the bilayer displayed a much improved R_{rms} value of 0.4 nm. It is because the viscous PVP solution has filled up the valley region of the AlO_x layer during spin-coating. Moreover, according to Fig. 2b the contact angles measured on the bilayer (left) indicated that the surface state of the bilayer is more hydrophobic (with lower surface energy) than that of the single AlO_x layer (right), exhibiting ~70 and 36° for the bilayer and AlO_x, respectively. It is because the cross-linked PVP surface has a much lower density of surface hydroxyl (OH-) groups than the surface of the untreated polar AlO_x. The dielectric surface states clearly influence the crystalline growth of organic channels.[13]

The XRD and AFM results from three different organic films

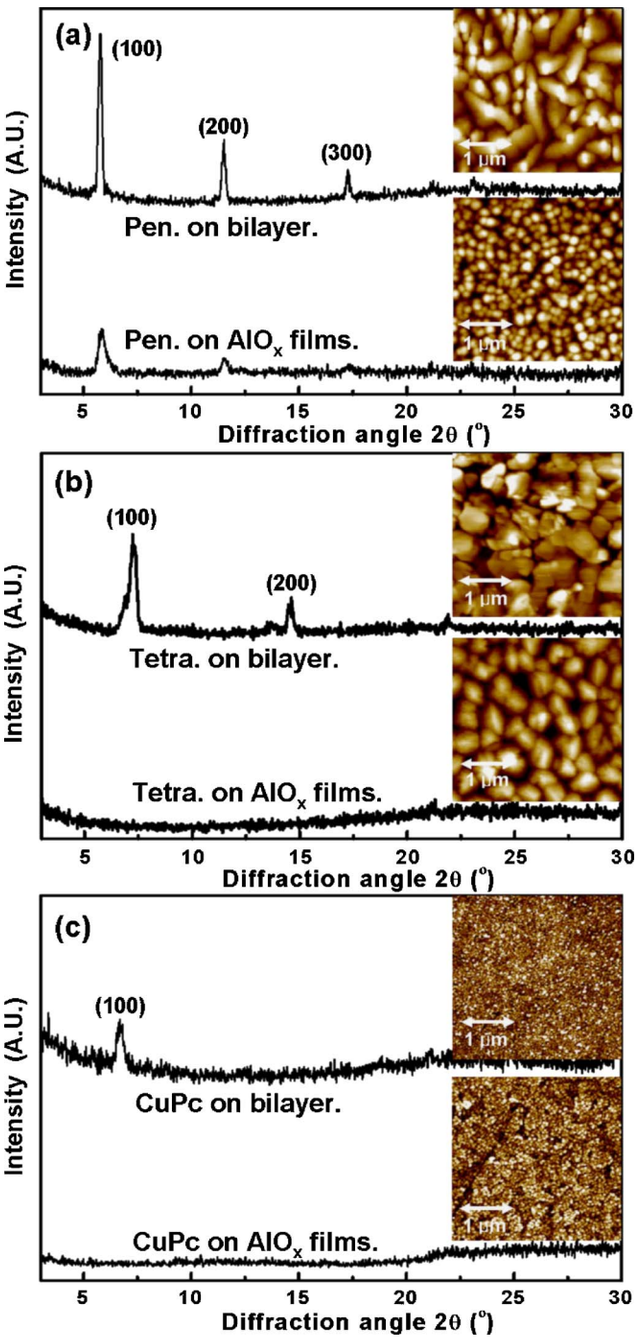

Figure 3. (Color online) XRD patterns and AFM surface images of (a) pentacene, (b) tetracene, and (c) CuPc films deposited on PVP (45 nm)/AlO$_x$ (100 nm)/ITO glass and on bare AlO$_x$ (100 nm)/ITO glass substrates, respectively.

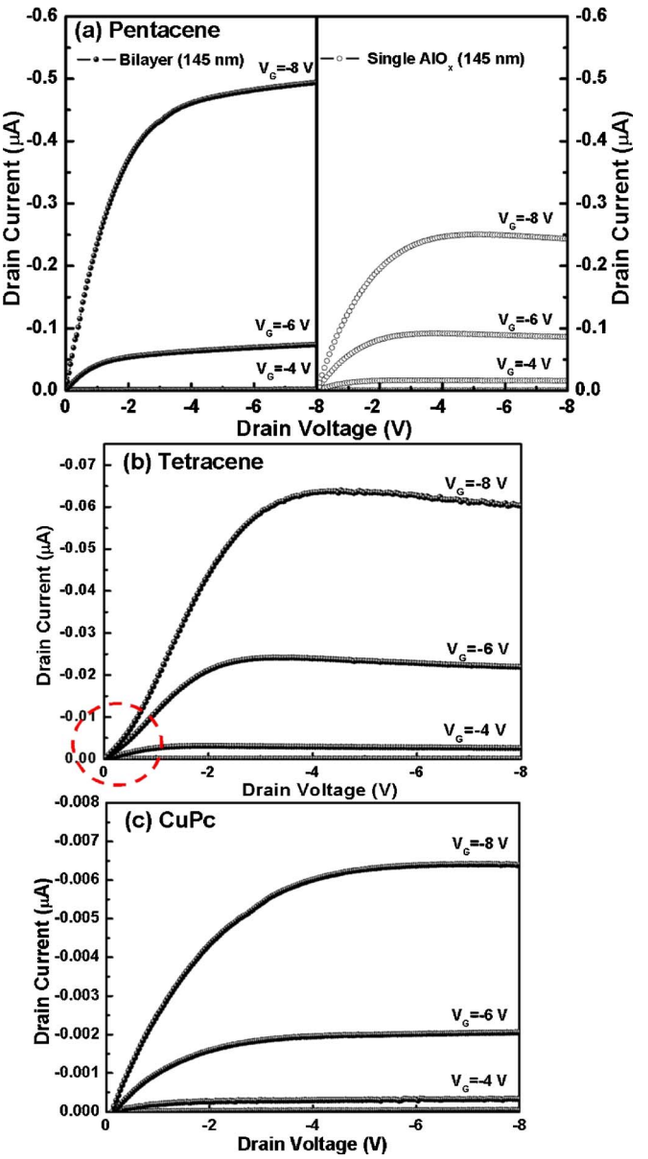

Figure 4. Output characteristics (I_D vs V_D) of (a) pentacene-, (b) tetracene-, and (c) CuPc-based TFTs with bilayer. Right side of a also shows the output characteristics of a reference pentacene-TFT with a bare single AlO$_x$ layer of 145 nm thickness.

grown on the bilayer and bare single AlO$_x$ layer are shown in Fig. 3a-c. For the organic layers grown on the bare AlO$_x$, the tetracene and CuPc films exhibited no diffraction peaks at all while weak diffraction peaks appeared in the case of pentacene. In contrast, all the organic layers grown on the PVP/AlO$_x$, bilayer display very good crystalline order. This is because the smooth PVP overlayer was in a hydrophobic state, which is known to help organic molecules to grow well in a crystalline phase during deposition.[11] In particular, the pentacene film, well known to grow with an orientation parallel to the c*-axis,[14,15] exhibited much higher crystalline quality than the other organic films (tetracene and CuPc). The insets of Fig. 3a-c show the individual AFM images of the three organic active layers grown on the bilayer and the single AlO$_x$ layer. According to the AFM surface images, the pentacene and tetracene exhibit larger organic grains as deposited on the bilayer than as deposited on the single AlO$_x$ layer, while the substrate effect has not been clearly observed in the AFM image for the CuPc layer growth. Based on the present results from the C–V, J–E, XRD, and AFM measurements, we chose the PVP/AlO$_x$ bilayer as our key dielectric to fabricate low-voltage driven OTFTs, because no good crystalline organic channel is expected from the single high-k AlO$_x$ layer, and also because low-voltage operation of OTFTs was not compatible with the low-k PVP layer due to its high leakage current.

The drain current–drain voltage (I_D–V_D) output characteristics of our OTFTs with the bilayer dielectric of 145 nm thickness are displayed in Fig. 4a-c for pentacene-, tetracene-, and CuPc-organic channels, respectively. (For pentacene-channels, we also showed the

output characteristics of a reference OTFT with a single 145 nm thick AlO_x dielectric.) According to Fig. 4a, pentacene-based TFT with the bilayer (left) exhibited the saturation current of 0.5 μA that is two times higher than that of TFT with the AlO_x single layer (right) under a same gate bias (V_G) of −8 V. It is worthy of note because the single dielectric layer possesses quite higher capacitance than that of the bilayer according to Fig. 1b. These results can be explained by considering the high-quality crystalline growth of pentacene on the smooth hydrophobic PVP overlayer as discussed in previous figures (Fig. 2a and b and Fig. 3a); here, the channel/dielectric interface and channel crystalline quality become more important for drawing I_D current than just the magnitude of dielectric capacitance. For the tetracene- and CuPc-based TFTs with the bilayer the maximum current was only 0.06 (Fig. 4b) and 0.006 μA (Fig. 4c), respectively, because their hole mobilities are basically lower than that of the pentacene-based TFTs.[16-18] In particular, nonohmic behavior is noted from the tetracene-based TFT, as indicated by a dotted circle at an initial V_D stage (Fig. 4b). This is because the highest occupied molecular orbital (HOMO) level of tetracene is much deeper than those of pentacene and CuPc, acting as an injection barrier against the holes from the Au electrode.[19] In general, it is interesting to find that the tetracene- and CuPc-based TFTs appear to operate well even under the same low gate bias of −8 V despite their intrinsic or extrinsic drawbacks. We may thus regard that our polymer/AlO_x bilayer possesses sufficiently high capacitance for low-voltage OTFT operation as well as an optimum surface condition for channel interfacing.

The drain current–gate bias (I_D–V_G) relationships obtained under the saturation-regime drain-source biases (V_{DS}) from our OTFTs are displayed in Fig. 5a-c. The pentacene OTFT with our bilayer dielectric exhibited a good field-effect mobility of 0.55 cm^2/V s, a high on/off current ratio of $\sim 5 \times 10^5$ subthreshold swing (SS) of ~0.5 V/dec, and threshold voltage (V_T) of ~−5 V, while the TFT with a single AlO_x layer showed relatively lower mobility of 0.17 cm^2/V s and inferior SS of ~0.7 V/dec (Fig. 5a). The tetracene- and CuPc-based OTFT appeared to possess lower field mobilities than those of pentacene-TFTs, showing their values of 0.07 and 0.004 cm^2/V s, respectively (see the transfer curves of Fig. 5b and c). As expected, the on/off current ratios of the tetracene- and CuPc-based OTFTs were also lower than those of the pentacene TFTs, at $\sim 5 \times 10^4$ and $\sim 10^3$, respectively. Because the reported typical field mobilities of tetracene, pentacene, and CuPc OTFTs were ~0.7, ~ 0.1, and ~0.004 cm^2/V s at room temperature our presented values achieved using the bilayer dielectric (0.55, 0.07, and ~0.004 cm^2/V s) are not only quite comparable to those of other groups[16-18] but also potentially more meaningful in that ours were achieved under a low operating voltage while previously reported values were obtained under high voltages over 30 V.

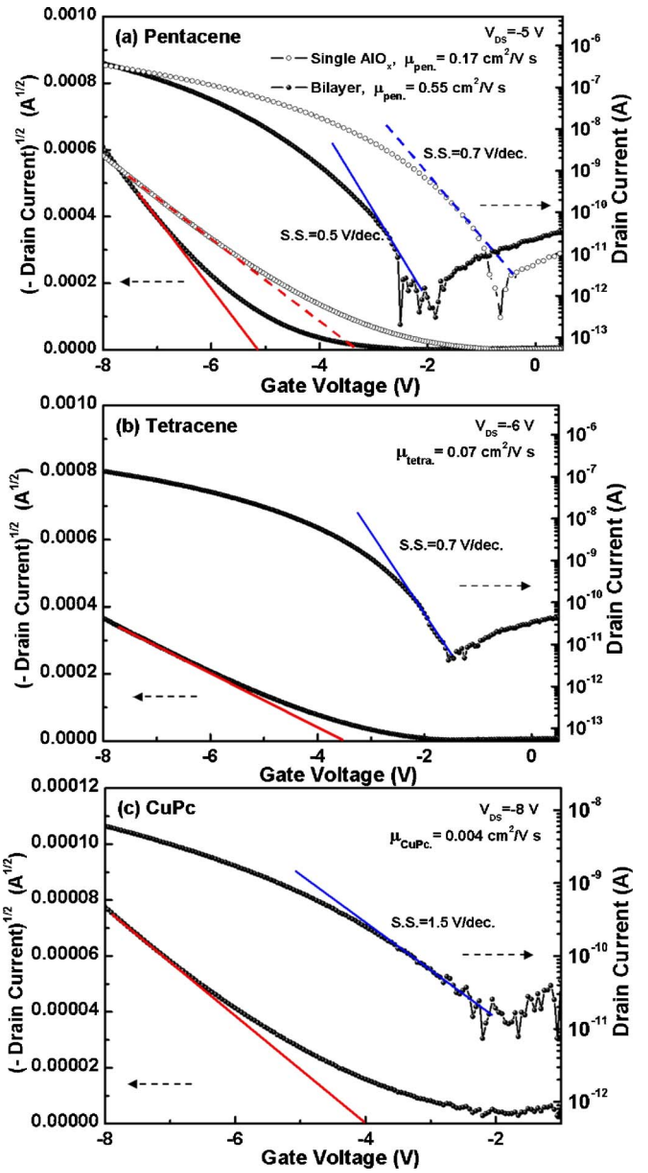

Figure 5. (Color online) $\sqrt{-I_D}$ vs V_G and log ($-I_D$) vs V_G transfer curves obtained from OTFTs adopting (a) pentacene channel at $V_{DS} = -5$ V, (b) tetracene channel at $V_{DS} = -6$ V, and (c) CuPc channel at $V_{DS} = -8$ V.

Conclusions

We have fabricated OTFTs with various organic channels but with a thin common PVP/AlO_x bilayer dielectric. Quite a large capacitance of 31 nF/cm^2 and a high dielectric strength of ~4 MV/cm were achieved from the thin PVP/thick high-k oxide bilayer dielectric film. Organic channels on the bilayer showed good crystalline quality, which was attributed to the hydrophobic and smooth PVP overlayer on the rough hydrophilic AlO_x. Our pentacene-, tetracene-, and CuPc-based OTFTs with the bilayer exhibited reasonable field-effect mobility values of ~0.55, 0.07, and ~0.004 cm^2/V s, respectively, operating at a low voltage of less than −8 V. We conclude that these low-voltage performances are mainly attributed to the polymer/AlO_x bilayer dielectric approach that enabled us to synthesize good crystalline organic channels and achieve quite a high effective dielectric capacitance without losing the overall dielectric strength.

Acknowledgments

This research was performed with financial support from KOSEF (program no. M1-0214-00-0228) and LG Philips LCD (project year 2005). They also acknowledge support from the Seoul Science Fellowship and Brain Korea 21 Project. J.H.K. acknowledges the financial support of the eSSC at Postech funded by MOST/KOSEF.

Yonsei University assisted in meeting the publication costs of this article.

References

1. F. Eder, H. Klauk, M. Halik, U. Zschieschang, G. Schmid, and C. Dehm, *Appl. Phys. Lett.*, **84**, 2673 (2004).
2. H. E. A. Huitema, G. H. Gelinck, J. B. P. H. van der Putten, K. E. Kuijk, C. M. Hart, E. Cantatore, P. T. Herwig, A. J. J. M. van Breemen, and D. M. de Leeuw, *Nature (London)*, **414**, 599 (2001).
3. L.-L. Chua, R. H. Friend, and P. K. H. Ho, *Appl. Phys. Lett.*, **87**, 253512 (2005).
4. A. Facchetti, M.-H. Yoon, and T. J. Marks, *Adv. Mater. (Weinheim, Ger.)*, **17**, 1705 (2005).
5. J. Puigdollers, C. Voz, A. Orpella, R. Quidant, I. Martin, M. Vetter, and R. Alcubilla, *Global Ecol. Biogeogr.*, **5**, 67 (2004).

6. J. Veres, S. D. Ogir, S. W. Leeming, D. C. Cupertino, and S. M. Khaffaf, *Adv. Funct. Mater.*, **13**, 199 (2003).
7. H. Klauk, M. Halik, U. Zschieschang, G. Schmid, W. Radlik, and W. Weber, *J. Appl. Phys.*, **92**, 5259 (2002).
8. R. Parashkov, E. Becker, G. Ginev, T. Riedl, H.-H. Johannes, and W. Kowalsky, *J. Appl. Phys.*, **95**, 1594 (2004).
9. I. N. Hulea, S. Russo, A. Molinari, and A. F. Morpurgo, *Appl. Phys. Lett.*, **88**, 113512 (2006).
10. T. Ohta, T. Nagano, K. Ochi, Y. Kubozono, E. Shikoh, and A. Fujiwara, *Appl. Phys. Lett.*, **89**, 053508 (2006).
11. D. K. Hwang, K. Lee, J. H. Kim, S. Im, C. S. Kim, H. K. Baik, J. H. Park, and E. Kim, *Appl. Phys. Lett.*, **88**, 243513 (2006).
12. D. K. Hwang, K. Lee, J. H. Kim, S. Im, J. H. Park, and E. Kim, *Appl. Phys. Lett.*, **89**, 093507 (2006).
13. J. Veres, S. Ogier, G. Lloyd, and D. D. Leeuw, *Chem. Mater.*, **16**, 4543 (2004).
14. F.-J. M. Z. Heringdorf, M. C. Reuter, and R. M. Tromp, *Nature (London)*, **412**, 517 (2001).
15. K. Itaka, M. Yamashiro, J. Yamaguchi, M. Haemori, S. Yaginuma, Y. Matsumoto, M. Kondo, and H. Koinuma, *Adv. Mater. (Weinheim, Ger.)*, **18**, 1713 (2006).
16. Y. Jin, Z. Rang, M. I. Nathan, P. P. Ruden, C. R. Newman, and C. D. Frisbie, *Appl. Phys. Lett.*, **85**, 4406 (2004).
17. D. J. Gundlach, J. A. Nichols, L. Zhou, and T. N. Jackson, *Appl. Phys. Lett.*, **80**, 2925 (2002).
18. Z. Bao, A. J. Lovinger, and A. Dodabalapur, *Appl. Phys. Lett.*, **69**, 3066 (1996).
19. J. Sworakowski and J. Ulanski, *Annu. Rep. Prog. Chem., Sect. C: Phys. Chem.*, **99**, 87 (2003).